Clim Dyn (2008) 30:455–465
DOI 10.1007/s00382-007-0306-1

Mechanisms for the land/sea warming contrast exhibited by simulations of climate change

Manoj M. Joshi · Jonathan M. Gregory · Mark J. Webb · David M. H. Sexton · Tim C. Johns

Received: 8 January 2007 / Accepted: 13 August 2007 / Published online: 11 September 2007

Abstract The land/sea warming contrast is a phenomenon of both equilibrium and transient simulations of climate change: large areas of the land surface at most latitudes undergo temperature changes whose amplitude is more than those of the surrounding oceans. Using idealised GCM experiments with perturbed SSTs, we show that the land/sea contrast in equilibrium simulations is associated with local feedbacks and the hydrological cycle over land, rather than with externally imposed radiative forcing. This mechanism also explains a large component of the land/sea contrast in transient simulations as well. We propose a conceptual model with three elements: (1) there is a spatially variable level in the lower troposphere at which temperature change is the same over land and sea; (2) the dependence of lapse rate on moisture and temperature causes different changes in lapse rate upon warming over land and sea, and hence a surface land/sea temperature contrast; (3) moisture convergence over land predominantly takes place at levels significantly colder than the surface; wherever moisture supply over land is limited, the increase of evaporation over land upon warming is limited, reducing the relative humidity in the boundary layer over land, and hence also enhancing the land/sea contrast. The non-linearity of the Clausius–Clapeyron relationship of saturation specific humidity to temperature is critical in (2) and (3). We examine the sensitivity of the land/sea contrast to model representations of different physical processes using a large ensemble of climate model integrations with perturbed parameters, and find that it is most sensitive to representation of large-scale cloud and stomatal closure. We discuss our results in the context of high-resolution and Earth-system modelling of climate change.

Keywords Climate change · Climate models · Surface temperature · Climate sensitivity

M. M. Joshi · J. M. Gregory · M. J. Webb · D. M. H. Sexton · T. C. Johns
Met Office Hadley Centre, Exeter, UK

M. M. Joshi (✉) · J. M. Gregory
Walker Institute for Climate System Research, Department of Meteorology, University of Reading, Earley Gate, PO Box 243, Reading RG6 6BB, UK
e-mail: m.m.joshi@reading.ac.uk

1 Introduction

It is well known that in climate model simulations of transient climatic warming over the twenty-first century, land areas on average warm more rapidly than the oceans; we refer to this phenomenon as "the land/sea contrast" in temperature change. Since the land surface is where human societies are located, understanding the land/sea contrast is of considerable relevance to predicting the impacts of global warming. The land/sea contrast occurs partially as a result of the different thermal inertias of the land and ocean, with the latter mixing heat more readily away from the surface than the former. However, it is seen also in simulated equilibrium responses of land and ocean to climate perturbations. For instance, in a standard experiment with an atmospheric general circulation model coupled to a "slab" or "mixed-layer" ocean (henceforth we refer to this configuration as a "slab GCM"), forced by doubling CO_2 and run to equilibrium, the warming in the globally averaged land temperature is more than the warming in the globally averaged ocean temperature (e.g. Manabe et al. 1991; Senior and Mitchell 1993). The extra warming over land occurs despite land and ocean receiving a similar

radiative forcing perturbation. The situation is clarified in Fig. 1.

In this paper we quantify the land/sea contrast in climate change projections using a number of atmosphere-ocean general circulation models (AOGCMs). We employ a conceptual model and idealised experiments to explain how the land/sea contrast can initially develop. Finally we investigate which physical processes are most important in amplifying the land/sea contrast using an ensemble of equilibrium climate change experiments, with each ensemble member having a different parameter perturbed.

2 The land/sea contrast in scenarios of increased greenhouse gases

The magnitude of the land/sea contrast, which we shall define in this paper as the average warming over land divided by average warming over sea, is shown in Fig. 2 from a number of AOGCM simulations following the SRES A1B emissions scenario, made available for the IPCC 4th assessment report (AR4). The lines show that the land/sea contrasts are always greater than 1, the average across AOGCMs of these time-mean ratios is 1.53, and their standard deviation is 0.13. During the time-dependent climate change of the twentieth century, land areas have warmed on average more than sea areas, with the observed land/sea ratio lying within the ranges produced by AOGCM simulations of twentieth century climate change (Sutton et al. 2007).

The time-variation of the land/sea contrast in any AOGCM is considerably less than the spread among AOGCMs (Fig. 2). The mean across AOGCMs of the

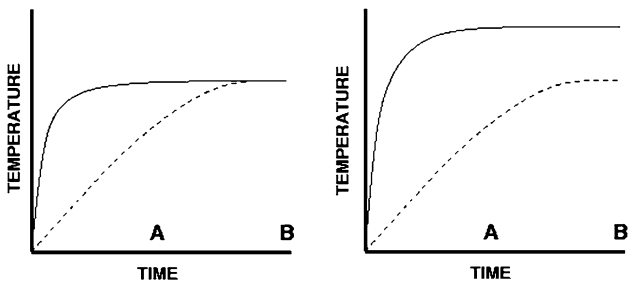

Fig. 1 Temperature evolution under a radiative forcing that is switched on at time $t = 0$ and kept constant. In *both panels* the *solid line* is the evolution of the land temperature and the *dashed line* represents the ocean temperature. The *left hand panel* shows the evolution of land temperature (*solid*) and ocean temperature (*dashes*) with no equilibrium land/sea contrast. At time A, the land temperature has risen by more than the ocean temperature because of the lower thermal inertia of the former. However, by time B, the ocean has warmed up to the same degree as the land. The right hand panel shows the scenario with an equilibrium land/sea contrast. At time B, the land is still warmer than the ocean, despite both land and ocean being in equilibrium with the new radiative forcing

decadal standard deviation in the land/sea contrast is only 0.05. Huntingford and Cox (2000) drew attention to the constancy of the land/sea contrast in HadCM3, without suggesting a physical explanation. The land/sea contrast in some of the same atmosphere GCMs coupled to slab ocean models, in steady state double-CO_2 climates, are shown as symbols on the right-hand side of Fig. 2. (Cf Sutton et al. 2007, who compare idealised scenarios of increasing CO_2 with constant doubled CO_2 in AOGCMs.) As in the schematic picture of Fig. 1, these numbers are also greater than 1. The equilibrium value of the land/sea contrast in any particular slab GCM is smaller than the transient value in its AOGCM counterpart, and the mean value across slab GCMs is 1.37 (cf: 1.53 in AOGCMs), suggesting that the differing thermal inertias of land and ocean, whilst certainly being important contributors to the transient land/sea contrast in AOGCMs, are not the dominant effect. Manabe et al. (1991) found a similar result when comparing the land/sea warming contrast between 2×CO2 and 1×CO2 slab GCM integrations with the land/sea warming contrast between the start and the end of the twenty-first century in a coupled ocean-atmosphere simulation.

It is reasonable to assume that some component of the land/sea contrast is associated with the different Bowen ratios (ratio of sensible heat flux to latent heat flux) over land and sea. However, as we shall see, this fact does not explain why moisture in both the soil and the boundary layer over land is restricted when a warming climate perturbation is applied.

Some of the land/sea contrast in temperature change can be related to summer drying in continental areas in the midlatitudes (e.g. Manabe et al. 1992; Rowell and Jones 2006). The drier soil leads to a drier boundary layer, less cloud, more shortwave radiation (henceforth "SW") reaching the surface, and a warmer surface. Local feedbacks of this kind will doubtless have an influence, and the model spread in the land/sea contrast may be symptomatic of the different amplitudes of the feedbacks in the different models (Sect. 6). However, the land/sea contrast is evident at most latitudes (Huntingford and Cox 2000; Cubasch et al. 2001, Fig. 14.10; Sutton et al. 2007), suggesting that a more widespread mechanism may be involved.

3 The land/sea contrast in a +4K experiment

The land/sea contrast could be caused by climate feedbacks generally being more positive over land. Using time-averaged radiative fluxes at the top of the atmosphere (henceforth "TOA"), (Boer and Yu 2003; Figs. 3, 4) have studied the geographical distribution of the climate feedback parameter, but remarkably it shows no evidence for a land/sea contrast, despite the land/sea contrast being the

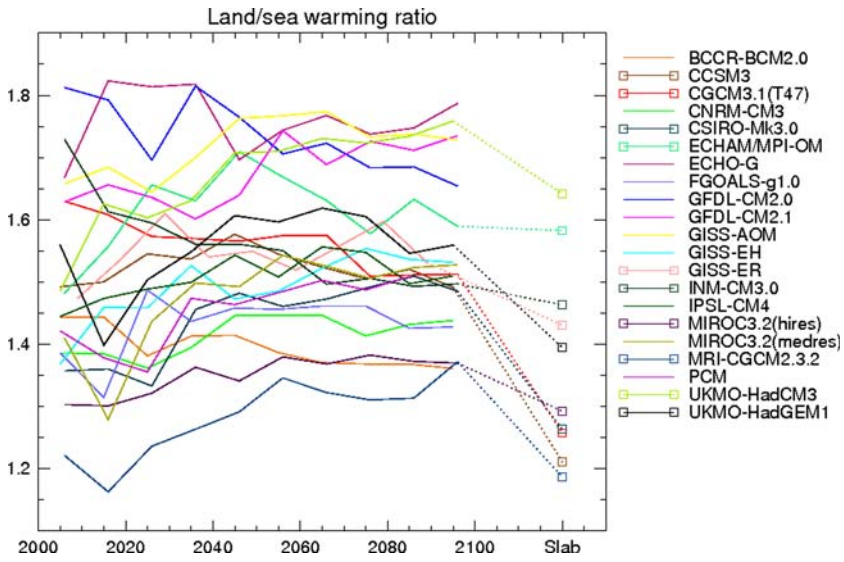

Fig. 2 The land/sea contrast (again, defined in this paper as land warming *divided by* ocean warming) in some IPCC AR4 GCMs. The *solid lines* show the time-variation of the land/sea contrast in a number of AOGCMs. The *symbols* on the right hand side show the land/sea contrast in corresponding slab GCMs, and are colour-coded to be the same models as the transient curves

most notable geographical feature of the surface temperature change.

Alternatively the land/sea contrast might be caused by CO_2 radiative forcing being generally greater over land. However, calculations of TOA CO_2 radiative forcing do not support this possibility (e.g. Boer and Yu 2003; Fig. 2). There is a land/sea contrast in anthropogenic aerosol forcing, but this is an effect which tends to reduce the warming over land, where the aerosol is emitted.

We confirm that the land/sea contrast does not relate to TOA radiative forcing or feedback by reference to the experiment illustrated in Fig. 3 (top panel), which shows the difference in surface temperature between a 5-year (1978 and 1983) control experiment (called "AMIP") of the HadGAM1 model (Martin et al. 2006) with monthly averaged SST from observations as the lower boundary condition of the model, and a perturbation experiment (called "AMIP+4 K") in which 4 K is added uniformly to the SST. This kind of perturbation experiment is commonly used to measure climate feedback parameters (e.g.: Cess et al. 1990). In this experiment, there is no externally imposed radiative forcing—the only way the land can be heated is by advection from the +4 K ocean. The result is that the land warms rapidly (within about a month) by more than 4 K. The land/sea contrast in this experiment is $\sim$1.4, which is similar to the land/sea contrast obtained from a standard "control" and "2×CO_2" slab version of HadGAM1 (Johns et al. 2006). The similarity of these results suggests that much of the land/sea contrast in 2×CO_2 experiments is driven by local feedbacks related to warming, rather than by different effects of CO_2 forcing over land and sea. In a parallel experiment in which SST is lowered by 4 K compared to the control, the land temperature falls by more than 4 K (ratio of land/ocean cooling is $\sim$1.3, Fig. 3, bottom panel). Any explanation of the land/sea contrast must therefore also explain why cooling as well as warming is amplified on land.

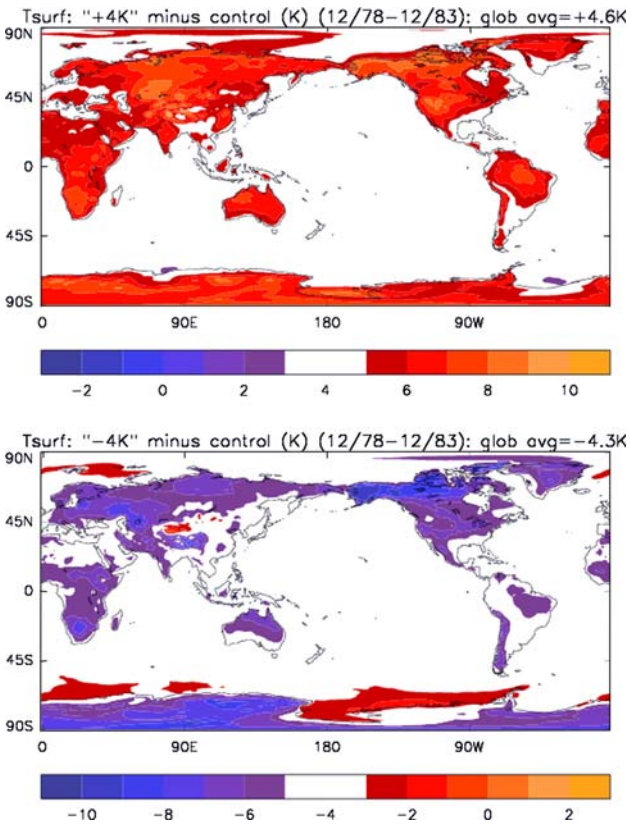

Fig. 3 Five-year averaged surface temperature difference between a control HadGAM1 experiment and a perturbation experiment with +4 K SSTs (*top*) and –4 K SSTs (*bottom panel*). Note that the white contours represent 3–5 K (*top*) and –5 to –3 K (*bottom*)

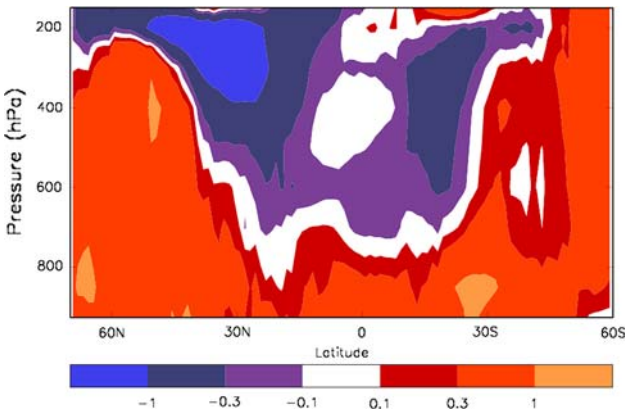

Fig. 4 Zonal cross section of temperature difference between land and ocean points between the "AMIP" and "AMIP+4 K" experiments

4 The initial perturbation: a conceptual model

In this section, we propose a conceptual model to explain the origin of the land/sea contrast. The model has three elements: the existence of a level *CH* in the atmosphere at which there is no land/sea contrast in climate change; a change in lapse rate from the surface up to level *CH* when climate is perturbed, despite unchanged relative humidity (RH); the effects of a change in RH in the lower troposphere. (While *CH* does vary spatially in reality, we treat it as constant in the conceptual model.) In the next section, we demonstrate the elements of the conceptual model with GCM results.

4.1 Existence of level *CH*

For the first element of the conceptual model, we suggest that climate anomalies are transported efficiently around the world above level *CH*, making climate change a globally connected phenomenon, while below level *CH*, lapse rate and surface temperature are dominated by local feedbacks. Obviously this is an idealisation, but it resolves a paradox. On the one hand, it is found that local processes are important in determining local climate change, as in the land/sea contrast and the enhancement of high-latitude surface warming by sea ice or snow retreat. On the other hand, the large-scale geographical patterns of climate change in any given model are only weakly affected by the nature of the forcing; greenhouse gases and aerosols, which have different forcing patterns, produce similar land/sea contrast and high-latitude amplification. We suggest that heat transport above level *CH* causes the global average radiative forcing to be experienced everywhere, while processes below level *CH* are responsible for the local climate change. This suggests that the TOA diagnostics of Boer and Yu (2003) are relevant to the global radiation balance, but will not explain the patterns of surface climate change.

4.2 Lapse rate in the lower troposphere

The second element of the conceptual model is the effect of moisture on humidity and lapse rate. If the lapse rate $\Gamma \equiv -dT/dz$ were a constant, where T is air temperature and z altitude, the warming at level *CH* would be +4 K, the same as imposed at the sea surface. The dry adiabatic lapse rate is a constant $\Gamma_D = 9.8$ K km^{-1}, but atmospheric profiles over the sea are often saturated, so the time-averaged lapse rate Γ_O is less than Γ_D because the saturated adiabatic lapse rate Γ_S is less than Γ_D (e.g.: Holton 1992, p.290). The exponential increase in saturation specific humidity q_S with temperature at constant pressure (due to the Clausius–Clapeyron relationship) causes the saturated lapse rate Γ_S to decrease with increasing q_S. This means that Γ_S decreases with increasing temperature ($d\Gamma/dT < 0$), and for a given frequency of saturated cases, so does Γ_O. Hence the lapse rate changes by $\Delta\Gamma_O < 0$ when the climate is warmed, and the warming at level *CH* is greater than at the surface by $z(CH)^*|\Delta\Gamma_O|$.

We now invoke the conceptual model, which states that the warming over the land and the ocean are similar at level *CH*. Over the land, the warming aloft will increase the stability of the atmosphere and inhibit convection, causing the land surface temperature to rise until a new steady state is reached. When climate is warmed, q_S increases, so Γ_S decreases (again from Holton 1992, p.290). However, Γ_D, being independent of q_S, does not decrease. Since the time-averaged RH in the boundary layer over land is less than over the ocean, the time-averaged lapse rate over land (Γ_L) is closer to Γ_D, and so decreases less than Γ_O. Given uniform land/sea warming aloft at level *CH*, this implies that the land surface warms more than the ocean. Furthermore, the land tends to be warmer on average than the ocean. Because $d^2\Gamma_S/dT^2 > 0$, the change in Γ_S over land due to increasing temperature will be less than over ocean when climate is warmed. For both reasons, the reduction $|\Delta\Gamma_L|$ in the lapse rate over the land due to the presence of moisture will be smaller in magnitude than the reduction over the sea, so the land surface will warm by $z_C|\Delta\Gamma_O - \Delta\Gamma_L|$ more than the 4 K warming imposed at the sea surface.

To illustrate the effect, we consider the case in which the temperature at 3 km is changed from 280 to 281 K. Γ_L in the boundary layer is then calculated for different boundary layer RH values, assuming that RH $\approx$ frequency of saturated parcels (i.e.: unsaturated parcels have an RH of 0), so that the lapse rate $\Gamma_L \approx 0.5(\mathrm{RH} \times \Gamma_S + (1.0 - \mathrm{RH}) \times \Gamma_D)$ (using the same notation as Sect. 4.2). We integrate

downwards from 3 km to calculate the surface temperature change dTs. When RH = 0.7, dTs is 0.78 K; when RH = 0.65, dTs is 0.79 K; however, when RH = 0.2 (representative of very arid boundary layers), DT is 0.94 K, showing that the lapse rate effect enhances the land/sea contrast most in arid regions.

A land/sea contrast in temperature change can therefore occur solely through the nonlinearity of Γ with q, and the difference in RH between ocean and land. Next we show how RH can change over land when climate is perturbed, having a further influence on the land/sea contrast.

4.3 Boundary layer moisture supply

The dependence of saturation specific humidity on temperature also has effects on how RH over land changes under climate change, and makes up the final element of the conceptual model. Consider a simple representation of the hydrological cycle: moisture is evaporated from the sea; some precipitates out, and the remainder is transported over land. In the real world, moisture convergence will occur at the different levels in the atmosphere; for now, we assume that all moisture convergence occurs at a certain level C. We emphasise here that this level C is not necessarily the same as the level CH described above, since the vertical profiles of heat and moisture transport are different to each other.

Precipitation P over land results from moisture convergence and from local evaporation E from land, and runoff R returns the moisture to the sea (all have units kg/m^2). At equilibrium we can consider the time-averaged moisture balance over a point of land as the following:

$$P = E + R \quad \text{and} \quad M = P - E \tag{1}$$

where M is the moisture convergence in kg/m^2 at level C. Integrating over the whole depth of atmosphere and soil, we have $M = R$ (i.e. whatever moisture converges on some region must be lost by runoff eventually). If $k \equiv E/R$, where $0 < k < \infty$, then $E = kR = kM$.

We assume that on average M is approximately proportional to the specific humidity q_C kg/kg at level C, because the magnitude of moisture transport, and hence its convergence M, should be approximately proportional to q_C. Hence we write $M = Ar_CQ_C$, where A is a constant, r_C is the relative humidity (%) and Q_C the saturation specific humidity (kg/kg) at level C. However, $M \propto q_C$ is only an average behaviour because M can be strongly affected by changes in circulation as well. We comment on the consequences of the assumption in the next section.

The moisture content of the boundary layer (BL) depends on evaporation from the surface and upward transport from BL to level C; we assume the latter to be proportional to $q_{BL} - q_C$, or $r_{BL}Q_{BL} - r_CQ_C$, where q_{BL}, r_{BL} and Q_{BL} are the specific humidity (kg/kg), relative humidity (%) and saturation specific humidity (kg/kg) in the boundary layer, respectively. Thus:

$$d(r_{BL}\ Q_{BL})/dt \propto E - B(r_{BL}Q_{BL} - r_CQ_C) \tag{2}$$

where B is a mixing coefficient. In the steady state, $d/dt = 0$. Hence

$$B(r_{BL}Q_{BL} - r_CQ_C) = E = Akr_CQ_C \tag{3}$$

When a perturbation causing climate warming is imposed, we assume that r_C is unchanged, given the tendency of GCMs to display approximately constant RH at most levels in the atmosphere under climate change, so

$$\begin{aligned} &B(r_{BL}\Delta Q_{BL} - r_C\Delta Q_C) = Akr_C\Delta Q_C \\ &\quad \Rightarrow \Delta Q_C/\Delta Q_{BL} = B/(B + Ak)\ r_{BL}/r_C \end{aligned} \tag{4}$$

Since Q is a function of temperature T and pressure, but the pressure at any given level changes little between the two climates, $\Delta Q_{BL} = \Delta T_{BL}\mathrm{d}Q/\mathrm{d}T(T_{BL})$ and similarly for level C. We have argued above that $\Delta T_C > \Delta T_{BL}$, but this is less important than the increase of saturation specific humidity (following the Clausius–Clapeyron equation) being strongly nonlinear with respect to temperature. Since C is significantly colder than the surface, $\mathrm{d}Q/\mathrm{d}T(T_C) < \mathrm{d}Q/\mathrm{d}T(T_{BL})$ and $\Delta Q_C < \Delta Q_{BL}$. With an unchanged r_C, (4) can hold if r_{BL} decreases (RH in the boundary layer over land decreases). A reduction in r_{BL} is a feature exhibited by GCMs.

There are other possible changes consistent with (4). First, A (related to the efficiency of moisture convergence by the large-scale circulation) could increase, but this cannot happen everywhere if r_C does not change. Second, B (related to the efficiency of vertical mixing) might decrease; the arguments of Held and Soden (2006) give some support to this as a general phenomenon, but we have not investigated its contribution over land. Third, k could increase, which would tend to happen if the soil dries, because runoff from gravitational drainage is a steeply increasing function of soil moisture content. On the other hand, GCM studies show that warmer climates tend to exhibit precipitation over land in shorter, more intense bursts (Cubasch et al. 2001), which would tend to increase surface runoff for a given amount of evaporation, and so decrease k. We find no general tendency in k in our results.

There is an initial increase in E associated with the climate warming perturbation. Because the moisture supply depends on Q_C and does not increase correspondingly, the soil moisture is depleted. If the soil moisture falls below the critical point, evaporation is restricted, and the BL gets

drier. In time, a new balance is reached, in which potential increases in E are restricted as a consequence of restricted moisture supply. Restricting E means that the land surface warms more, because a higher temperature is needed to increase sensible heat loss and thermal radiation to compensate for the restricted evaporative cooling. We note that the reduction in r_{BL} will increase Γ_L, and thus enhance the land/sea contrast further.

We have suggested mechanisms whereby the land/sea contrast may result from moisture convergence occurring away from the surface, the dependence of Γ on humidity, and the non-linear increase in Q with T. By reversing the signs of changes, this conceptual model also explains the land/sea contrast in cooling (see Fig. 3, bottom panel), which was a requirement set out in Sect. 3.

5 Validating the conceptual model from GCM output

5.1 Existence of level C

One now has to ask the question "how realistic is the conceptual model?" Given that the land/sea contrast is visible in any number of climate GCMs, we diagnose relevant quantities in the Hadley Centre model HadGAM1 to justify the use of the assumptions in the conceptual model.

The conceptual model first postulates the existence of level *CH* at which temperature change is the same over land and ocean. Figure 4 shows that this level occurs at about 700–800 hPa in the tropics, and slightly higher up in the midlatitudes. The apparent difference up to 300 hPa around 50°N is due to reduced warming over the sea due to a strong upper-tropospheric cooling in the north Pacific. The globally averaged values of temperature change over land and sea are shown in Fig. 5. The two curves coincide at the 4000 m level, or 600 hPa.

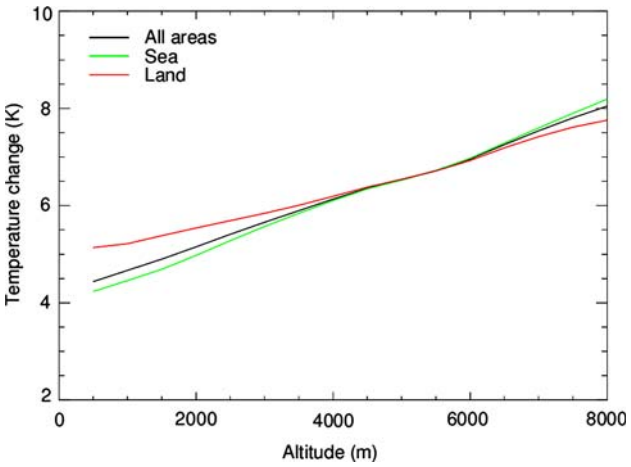

Fig. 5 Vertical profile of the area-averaged temperature difference between the AMIP and AMIP+4 K experiments: the land points are shown in *red* and the ocean points in *green*

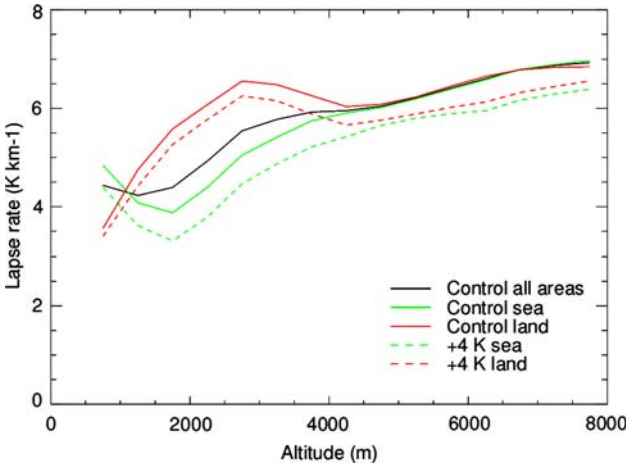

Fig. 6 The lapse rates in the HadGAM1 "AMIP" experiment (*solid*) and "AMIP+4 K" experiment (*dashed*). Land points are in *red*, ocean in *green* and all in *black*

5.2 Lapse rate in the free troposphere

The reduction of the lapse rate over both land and sea is evident from the fact that the warming at level *CH* ($\sim$6 K) is greater than at the surface (4.5 K). As expected, the reduction in lapse rate $|\Delta\Gamma|$ is greater over sea than land, not only near the surface, but throughout the depth of the atmosphere, as shown by a comparison of the solid and dashed curves in Fig. 6. This difference alone would cause a land/sea warming contrast. Figure 7 shows the spatial variation in the lapse rate change in the lower troposphere. Changes in lapse rates appear to be part of the explanation of enhanced warming on land in most of North America (especially in the west), low-latitude South America, southern Africa, northern Europe, Siberia and northern Australia.

5.3 Boundary layer moisture supply

The changes in the hydrological cycle proposed in the conceptual model suppose that the transport of moisture from ocean to land must take place away from the surface, so that the effect of the lapse rate can be significant. A longitude-latitude map of the pressure levels at which moisture convergence C is highest is shown in Fig. 8. We choose this diagnostic to represent C, the level at which all moisture convergence takes place in the conceptual model of Sect. 4.3. The magnitude of transport increases

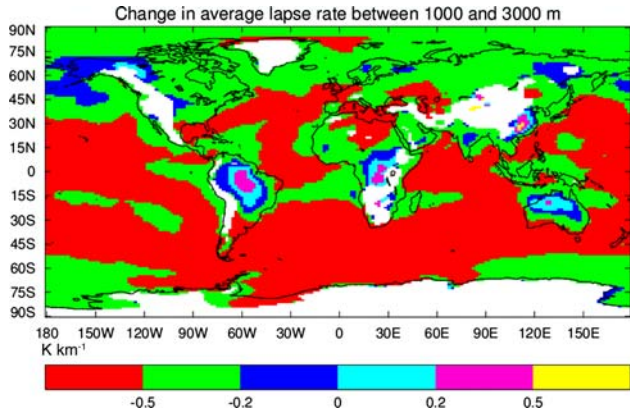

Fig. 7 A map of the change in lapse rate averaged over 1,000–3,000 m between the HadGAM1 "AMIP" and HadGAM1 "AMIP+4 K" experiments

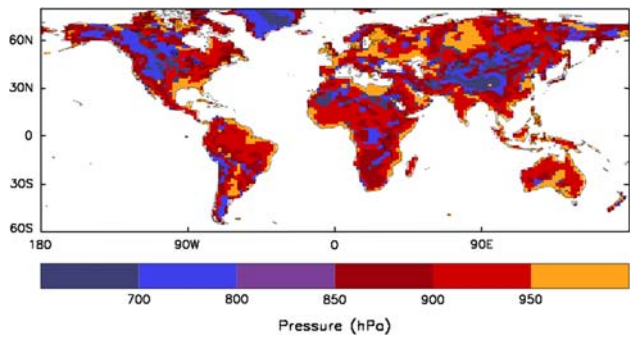

Fig. 8 Map of the pressure (hPa) at which the moisture convergence C reaches its highest value over land

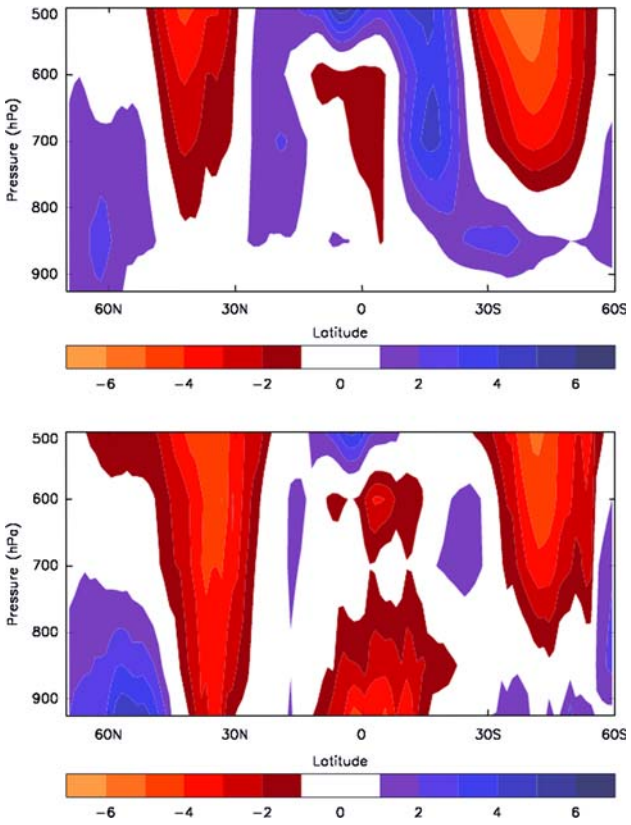

Fig. 9 Zonal cross section of change in relative humidity (%) over the oceans (*top panel*) and land (*bottom panel*) between the AMIP and "AMIP+4 K" HadGAM1 experiments

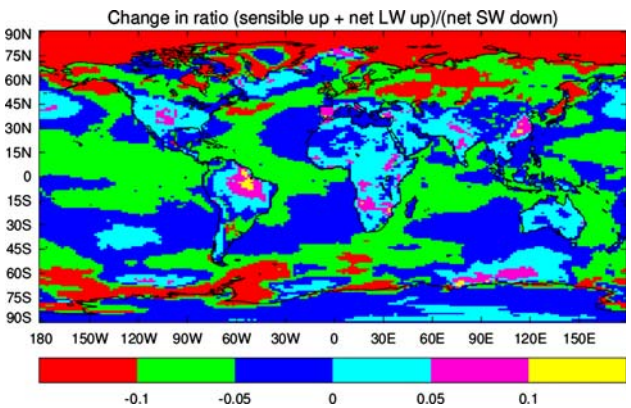

Fig. 10 The change in ratio of (upward sensible heat flux + net upward LW)/(net downward SW) between the "AMIP" and "AMIP+4 K" experiments

from the surface to a maximum at the 850–950 hPa region, somewhat lower than level *CH*, the level at which heat transport has eliminated the land/sea temperature contrast, because specific humidity falls off far more quickly with height than temperature. The pressure interval at which moisture transport takes place over land is consistent with the assumptions of the conceptual model above.

The conceptual model assumes that RH should be constant at level C and predicts a decrease in the boundary layer over land. Over the ocean, RH at 1.5 m is 81% in both the control and the +4 K cases. However, over land, RH at 1.5 m is 74% in the control case, and 71% in the +4 K case. The reduction in RH is intensified near the surface over land (see Fig. 9). The occurrence of the RH deficit within the land boundary layer, but not in the oceanic boundary layer, is consistent with the conceptual model.

Although evaporation E increases in some land areas where r_{BL} declines, the smaller r_{BL} may nonetheless indicate that the increase in E has been limited. We calculate the quantity $S \equiv$(upward sensible heat flux + net upward longwave radiative flux)/net downward shortwave radiative flux. We expect S to increase where E is restricted, and in such areas we expect enhanced surface warming. Figure 10 shows that this is indeed the case over land almost everywhere south of 45°N.

5.4 Dependence on the Clausius–Clapeyron relation

A crucial aspect of the conceptual model is the nonlinearity of the Clausius–Clapeyron equation with respect to temperature, causing evaporation at the land surface to outpace precipitation from the colder troposphere, and lapse rates to decline more strongly in the free troposphere over the sea than over the land. This aspect is tested quite simply by rerunning both the control and "+4 K SST" HadGAM1 experiments, with the Clausius–Clapeyron relationship for saturation specific humidity replaced by a linear function of temperature above 280 K. The threshold is chosen so that the relationship is only linear for those regions in the tropics beneath the 800 hPa level where moisture transport is significant (e.g. see Fig. 8). These two integrations are designated LIN and LIN+4 K.

The resulting profiles of temperature change over land and sea are shown in Fig. 11. The land/sea contrast is much smaller in "LIN+4 K minus LIN" case; indeed the globally averaged ratio is 1.05 (cf. 1.4 in the control case). The altered relationship for saturation specific humidity makes d^2q/dT^2 equal to zero above 280 K, and hence Γ less strongly dependent on T. This means that the differing lapse rate changes over ocean and land caused by climate warming does not happen. The change in lapse rates between LIN and LIN+4 K is shown in Fig. 12. When compared with Fig. 6, the difference between Γ(control) and Γ(+4 K) vanishes near the surface. In addition, there is reduced incidence of moisture limitation at the surface, again because d^2q/dT^2 is zero above 280 K. Area-averaged land RH at 1.5 m also shows less change between the LIN and LIN+4 K cases, being 74.5% in both cases, and S [=(upward sensible heat flux + net upward longwave radiative flux)/net downward shortwave radiative flux]

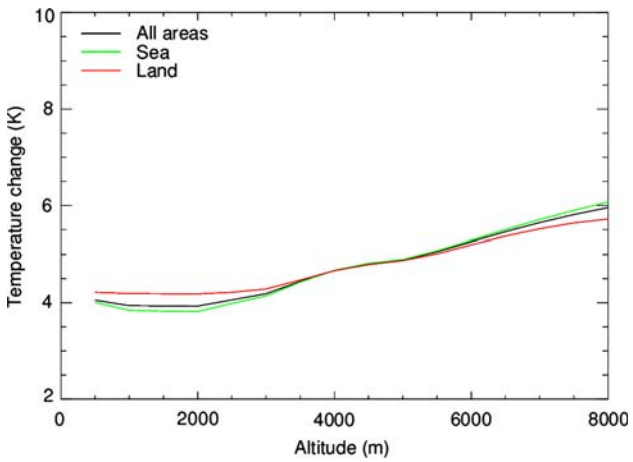

Fig. 11 Vertical profile of the area-averaged temperature difference between LIN+4 K and LIN experiments. Land points are shown in *red* and ocean points in green

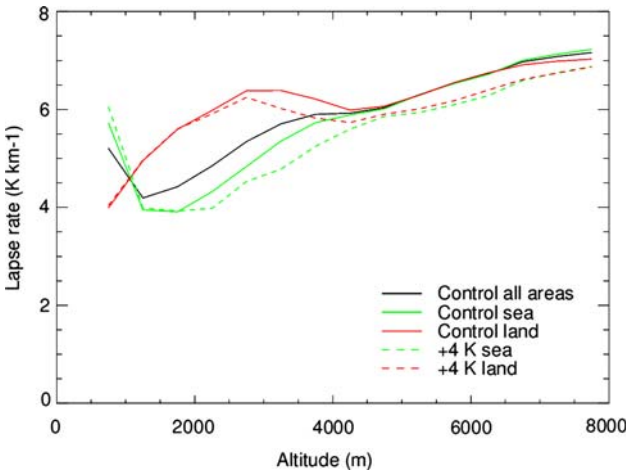

Fig. 12 The lapse rates in the HadGAM1 "LIN" experiment (*solid*) and "LIN+4 K" experiment (*dashed*). Land points are in *red*, ocean in *green* and all in *black*

likewise changes less than in the normal model. This result supports the hypothesis of the conceptual model than the non-linearity of the Clausius–Clapeyron equation is a major cause of the land/sea contrast when SST is perturbed.

The change of RH at 1.5 m over land in the AMIP case is illustrated in Fig. 13 (top panel), which shows change in RH vs RH over land points. At high values of RH, ΔRH is small (because sufficient moisture is available that evaporation is not greatly restricted upon warming), and the land/sea contrast is small (black points). When RH $< 40\%$, ΔRH is small (because the land is already quite dry and evaporation is already restricted in the control), but a small land/sea contrast exists (blue points) because of the lapse rate effect described in Sect. 4.2. At intermediate values of RH, ΔRH is high, and the land/sea contrast is high (mostly red/yellow points). This is the regime described in Sect. 4.3, and it is in this regime that feedbacks due to changes in cloud will occur (see next section). Figure 13 (bottom panel) shows ΔRH vs RH in the LIN and LIN+4 K experiments. ΔRH is much smaller than in the top panel, and there are relatively few blue, red and yellow points, consistent with a much smaller land/sea contrast.

The "LIN" experiments confirm that the land/sea contrast is not simply a result of a higher Bowen ratio over unsaturated land compared to ocean, because if it was, the land/sea contrast would still occur in the LIN+4 K run.

6 Cloud and other feedbacks

We have shown how the conceptual model is consistent with diagnostics from integrations of HadGAM1. Many of the regions that are affected by changes in tropospheric lapse rate are also affected by moisture limitation (see

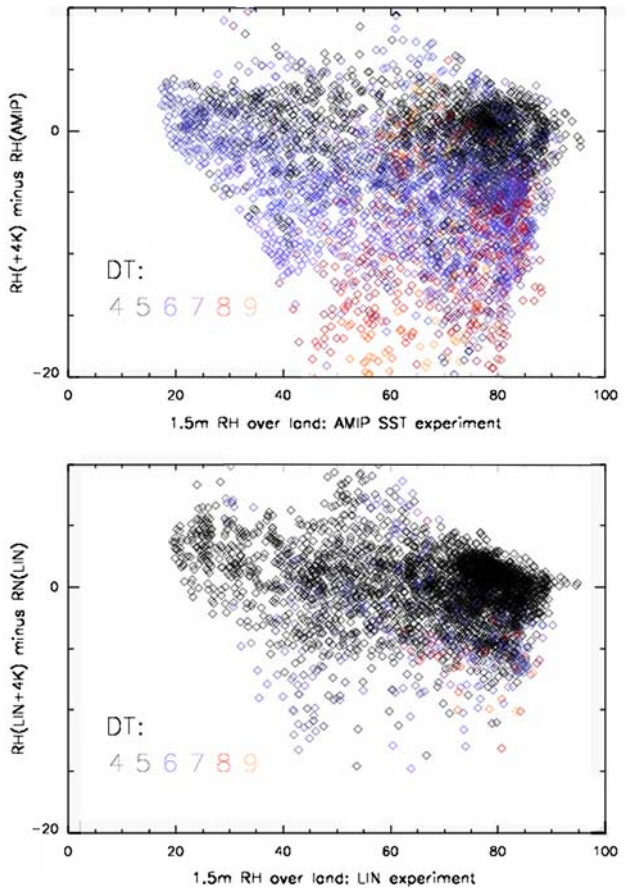

Fig. 13 RH at 1.5 m over land for all points between 45°N and 45°S in the AMIP SST experiment plotted against change in RH in the AMIP+4 K experiment (*top*). The *bottom panel* is as the *top panel* but for the LIN and LIN+4 K experiments. In each case a *colour coding* is applied to each model grid point representing its temperature rise

Table 1 Land/sea contrast and climate sensitivity in the QUMP SPP ensemble with having values of the land/sea contrast $<M - S$ or $>M + S$ where M is the mean of the ensemble (1.75) and S is the standard deviation (0.08)

QUMP ensemble member	Land/sea contrast	Climate sensitivity (K)
Control simulation	1.72	3.32
Stomatal resistance OFF (default ON)	1.57	2.95
Cloud droplet to rain conversion rate: 4×10^{-4} (default: 10^{-4})	1.58	3.91
Cloud droplet to rain conversion rate: 0.5×10^{-4} (default: 10^{-4})	1.88	2.84
Cloud fraction at saturation in boundary layer: 0.7 (default: 0.5)	1.92	2.53
Cloud fraction at saturation in free troposphere: 0.6 (default: 0.5)		
Cloud fraction at saturation in boundary layer: 0.8 (default: 0.5)	2.03	2.12
Cloud fraction at saturation in free troposphere: 0.65 (default: 0.5)		
Cloud droplet to rain conversion threshold-	1.84	3.10
land: 20×10^{-4} (default: 2×10^{-4}),		
sea: 5×10^{-4} (default: 0.5×10^{-4})		
Vertical gradient of cloud water in gridbox: ON (default: OFF)	1.95	2.57

Fig. 10), and together the two processes account for nearly all the locations where land/sea warming occurs. However, given its simplicity, the conceptual model does not explain fully the magnitude of the land/sea contrast. In the real world, or a GCM run under more realistic forcing, the land/sea contrast is influenced by a number of other physical mechanisms and feedbacks, which we now describe. In particular, the reduced RH that occurs over the land (see Fig. 9, bottom panel) leads to less cloud, and hence more solar radiation reaching the ground (e.g. Manabe et al. 1991).

In order to clarify which physical processes are most important, we examine the land/sea contrast in the QUMP (Quantifying Uncertainty in Model Prediction) ensemble of integrations carried out using 53 modified versions of the HadSM3 climate model (Williams et al. 2001), each with a model parameter perturbed to a low or high estimate based on observations and other studies (Murphy et al. 2004). HadSM3 consists of an earlier version than HadGAM1 of the Hadley Centre atmosphere GCM, coupled to a slab ocean model. Each version of the model is integrated to equilibrium using pre-industrial CO_2, and again with $2\times CO_2$.

Table 1 shows the experiments in which the land/sea contrast departs from the average value of the land/sea contrast in the ensemble (1.75) by more than one standard deviation (0.08). The perturbations in the experiments in Table 1 are (with one exception) those which modify the representation of clouds and precipitation, especially at low levels. The experiments with a large land/sea contrast are those with more cloud over land (and vice versa), suggesting that the large cloud amounts are more readily reduced in a warmed climate. Associated with the reduction in cloud amount is an increase in net downward SW at the surface. The difference in this quantity between the $2\times CO_2$ and $1\times CO_2$ runs described in Table 1 is shown in Fig. 14. Since increased surface SW causes warming, there is a more or less linear increase of land/sea contrast with downward SW.

There is one experiment in Table 1, which is not a cloud perturbation, and this is the "stomatal resistance turned off" experiment. The reason for the anomalously

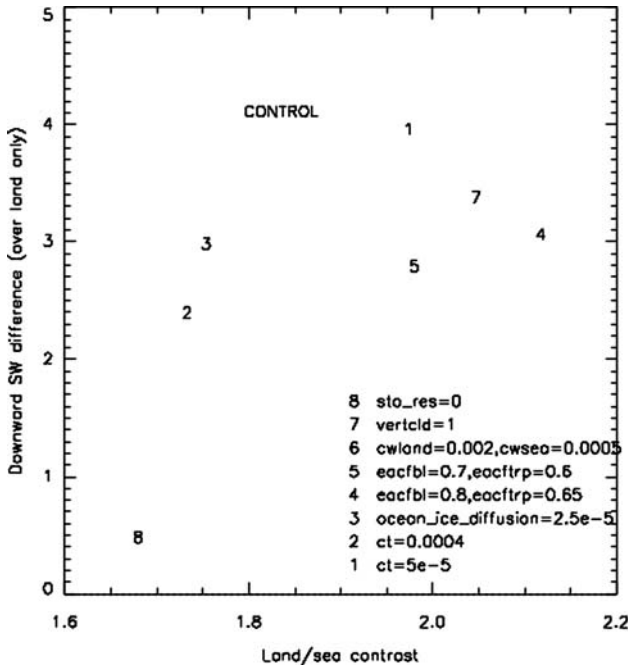

Fig. 14 Area-averaged change in downward surface SW over land only between 45°S and 45°N in the QUMP integrations where the land/sea contrast is more than 1 standard deviation away from the average value

low land/sea contrast can also be explained in terms of the conceptual model. In the standard HadSM3 set-up, stomatal resistance is on; that is to say, when CO_2 increases, stomata decrease in size, and transpiration, and thus surface evaporative cooling, is inhibited. The experiment with stomatal resistance turned off therefore allows more transpiration, more evaporative cooling of the surface for a given precipitation (i.e. k from Sect. 4.2 increases), and less warming on land. This effect of stomatal resistance will be absent from the +4 K integrations with HadGAM1, because it is a direct response to CO_2 in the atmosphere, which is not changed in those experiments.

There appears to be no significant relationship between equilibrium climate sensitivity and the land/sea contrast, although the reason for this might be the relatively small number of ensemble members. Future work will involve analysing the larger ensemble of Webb et al. (2006) with multiple parameter perturbations to reassess this lack of significance.

7 Coastal effects

There are coastal areas in the tropics where the land/sea contrast is very low in the AMIP/AMIP + 4 K simulations (Fig. 3). Flat coastal areas receive a disproportionate amount of moisture from small-scale circulations that transport moisture at levels very near to the surface, as shown in Fig. 8. At such levels the temperature difference between the surface and the level of moisture convergence may be small, so the change in specific humidity when climate is perturbed will be similar at both levels, and no moisture deficit occurs, or the air may be relatively moist, so the change in lapse rate is similar to that over the adjacent sea.

However, it is possible that the mechanism described above may lead to an underestimation of the land/sea contrast in coastal areas. As an example, consider a region in which moisture is advected from ocean to land with a certain profile in height. If this region is represented in a GCM by 1–2 grid points, moisture transport in the GCM will be dominated by diffusion rather than advection. The height profile of the GCM moisture transport will vary with q rather than uq, and will therefore be maximised closer to the surface than in reality. This will cause the C and CH levels from Sect. 4.1 to be closer to the surface in the GCM than in reality, thus potentially lowering the land/sea contrast in that region.

Locations such as western Europe, which is shown as experiencing virtually no land/sea contrast in warming in Fig. 3, have been shown to warm up more than the surrounding ocean in regional models (Jones et al. 1997). This dependence on resolution may also partially explain why earlier GCMs with far coarser resolution did not produce a significant land/sea contrast at low latitudes (Manabe et al. 1991). All these results suggest that high-resolution regional models should be used to verify climate model predictions of the magnitude of the land/sea contrast in coastal regions.

8 Conclusions

The land/sea contrast in surface warming is seen in transient and equilibrium climate change experiments, so is not just a result of the different thermal inertias of the ocean and land. We have proposed a conceptual model to show it can come about, and demonstrated some evidence in support of this with GCM results. The conceptual model has three elements: the existence of a level at which warming over land and sea is the same, the dependence of lapse rate on temperature and humidity, and a decrease in surface and boundary layer RH over land because of moisture limitation in unsaturated land areas caused by transport from the ocean occurring at levels significantly colder than the land surface. The lapse rate and hydrological changes depend on the nonlinearity of saturation specific humidity with respect to temperature in the Clausius–Clapeyron relationship, as shown by a minimal land/sea contrast in GCM experiments where q is a linear function of T above 280 K.

The effect of the dependence of lapse rate on temperature and humidity (Sect. 4.2) is to lower the lapse rate less over the land than the ocean, producing a larger warming over the land surface than over the ocean. The effect of moisture limitation in the boundary layer over land (Sect. 4.3) is to directly enhance land surface warming-this has the effect of raising the lapse rate over land as well.

The land/sea contrast is enhanced by reduction of cloud amount upon warming, and so its amplitude is dependent on the choice of parameters in climate models governing these changes. Analysis of the QUMP HadSM3 ensemble suggests that parameter changes that affect low cloud over the land give rise to the greatest land/sea contrast, because of the effect on net downward surface shortwave radiation. Enhancement of warming on land can also be caused by elevated CO_2 due to restriction of evaporation by stomatal closure. The magnitude of the land/sea contrast is not found to be generally related to climate sensitivity.

The results of the QUMP ensemble suggest that the land/sea contrast will be very sensitive to the way in which GCMs treat clouds in the boundary layer. Such treatments are becoming more complex (e.g. in HadGAM1), and will become even more complex in future, including the effects of chemical and aerosol interactions with low-level cloud. While including a more comprehensive range of processes improves the credibility of models in theory, differences in the implementation details from model to model may well enlarge the inter-model spread in the land/sea contrast (often taken as a measure of uncertainty). Examination of the sensitivity of evaporation and clouds to background RH changes in mesoscale models would help to reduce such uncertainty. In addition, diagnostics relevant to the conceptual model (such as those shown in Figs. 8 and 10, and the *A, B* and *k* terms in Eq. 4) should be examined in other AOGCMs, in order to confirm the generality of the results.

Examination of the land/sea contrast in the Hadley Centre global climate models has once again brought out changes in the hydrological cycle as being of crucial importance in determining transient and equilibrium temperature changes on land. Although there is quite rightly a move towards including more earth system components in attempting to improve predictions of the Earth's climate, the present work should reinforce the principle that reasonably faithful simulations of atmospheric dynamics, transport and hydrology are essential to the ability of a numerical model to properly predict responses to anthropogenic climate forcing.

Acknowledgments MJ, MW, DS and JG are supported by the UK Department for Environment, Food and Rural Affairs (Defra) contract number PECD/7/12/37. JG is supported by the National Centre for Atmospheric Science (NCAS). TJ is supported by the UK Government Meteorological Research (GMR) programme. We would like to thank the reviewers of the original submitted manuscript and Keith Shine for their useful comments. We acknowledge the modelling groups for providing their data for analysis for the AR4 and CFMIP, the Program for Climate Model Diagnosis and Intercomparison (PCMDI) for collecting and archiving the model output, and the JSC/CLIVAR Working Group on Coupled Modelling (WGCM) for organizing the model data analysis activity. The multi-model data archive is supported by the Office of Science, US Department of Energy.

References

Boer GJ, Yu B (2003) Climate sensitivity and response. Clim Dynam 20:415–429

Cess RD et al (1990) Intercomparison and interpretation of climate feedback processes in 19 atmospheric general circulation models. J Geophys Res 95:16601–16615

Cubasch U, Meehl GA, Boer GJ, Stouffer RJ, Dix M, Noda A, Senior CA, Raper SCB, Yap KS (2001) Projections of future climate change, in Climate Change 2001, the scientific basis. Contribution of working group 1 to the 3rd assessment report of the IPCC. Cambridge University Press, Cambridge, pp 525–582. ensembles of general circulation model simulations. Clim Dynam 27: 357–375

Held IM, BJ Soden (2006) Robust responses of the hydrological cycle to global warming. J Clim 16:5686–5699

Holton JR (1992) An introduction to dynamic meteorology. Academic, San Diego

Huntingford C, Cox PM (2000) An analogue model to derive additional climate change scenarios from existing GCM simulations. Clim Dynam 16:575–586

Johns TC et al (2006) The new Hadley Centre climate model HadGEM1: evaluation of coupled simulations. J Clim 19:1327–1353

Jones RG, Murphy JM, Noguer M, Keen AB (1997) Simulation of climate change over Europe using a nested regional climate model. II: Comparison of driving and regional model responses to a doubling of carbon dioxide. Quart J R Met Soc 123:265–292

Manabe S, Stouffer RJ, Spelman MJ, Bryan K (1991) Transient responses of a coupled ocean-atmosphere model to gradual changes of atmospheric CO_2. Part I: annual mean response. J Clim 4:785–818

Manabe S, Spelman MJ, Stouffer RJ (1992) Transient responses of a coupled ocean-atmosphere model to gradual changes of atmospheric CO_2. Part II: seasonal response. J Clim 5:105–126

Martin GM, Ringer MA, Pope VD, Jones A, Dearden C, Hinton TJ (2006) The physical properties of the atmosphere in the new Hadley Centre global environment model, HadGEM1. Part I: model description and global climatology. J Clim 19:1274–1301

Murphy JM, Sexton DMH, Barnett DN, Jones GS, Webb MJ, Collins M (2004) Quantification of modelling uncertainties in a large ensemble of climate change simulations. Nature 430:768–772

Rowell DP, Jones RG (2006) Causes and uncertainty of future summer drying over Europe. Clim Dynam 27:281–299

Senior CA, Mitchell JFB (1993) Carbon dioxide and climate: the impact of cloud parameterization. J Clim 6:393–418

Sutton RT, Dong B, Gregory JM (2007) Land/sea warming ratio in response to climate change: IPCC AR4 model results and comparison with observations. Geophys Res Lett 34:L02701

Webb MJ et al (2006) On the contribution of local feedback mechanisms to the range of climate sensitivity in two GCM ensembles. Clim Dynam 27:17–38

Williams KD, Senior CA, Mitchell JFB (2001) Transient climate change in the Hadley Centre models: the role of physical processes. J Clim 14:2659–2674